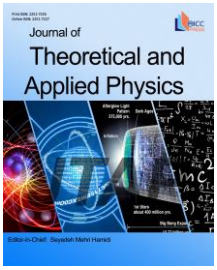

J. Theor. Appl. Phys 2026; 20(1): 45-54

Journal of Theoretical and Applied Physics (JTAP)

https://doi.org/10.57647/jtap.2026.2001.05

Research Article

Exploring Tl $_{1-x}$B $_x$As: A New Addition to the Family of Advanced Materials with Distinct Structural, Electronic and optical Properties

Zoulikha Abed*, Laid Abdelali, Abdelhadi Lachabi

Applied Materials Laboratory, Research Center, Sidi Bel Abbes University, 22000, Algeria

***Corresponding author:** zoulikhaabed3@gmail.com

Article History:

Received:
12 September 2025

Revised:
06 October 2025

Accepted:
13 November 2025

Published Online:
06 December 2025

Published in Issue:
28 February 2026

Abstract

In this study, we present a theoretical investigation of the structural, electronic, and optical properties of the ternary compound $Tl_{1-x}B_xAs$ ($0 < x < 1$) crystallizing in the zinc blende (ZB) structure, using density functional theory (DFT) within both the generalized gradient approximation (GGA) and the modified Becke–Johnson (mBJ-GGA) potential. The calculated results reveal that the crystal lattice maintains its structural stability across all studied boron concentrations. Within the GGA approach, the alloy exhibits a metallic nature with no distinct band gap between the valence and conduction bands. However, when the mBJ-GGA correction is applied a remarkable direct band gap emerges at the boron concentration of x = 0.75, highlighting its semiconducting behavior. From an optical point of view the imaginary part of the dielectric function indicates that the absorption edge starts from zero energy for low boron concentrations (x = 0.25 and 0.5) and extends up to around 8 eV while it shifts to approximately 10 eV for x = 0.75, indicating a wider absorption range. This broad optical response combined with structural stability and tunable electronic properties suggests that $Tl_{1-x}B_xAs$ alloys are promising materials for advanced technological applications particularly in optoelectronic and semiconductor–metal transition devices.

Keywords: $Tl_{1-x}B_xAs$alloys, Zinc-blende structure, Bulk modulus, Optical properties, Band gap enargy, DFT, GGA, MBJ-GGA, Dielectric function, Refractive index

Cite this article: Abed, Z., Abdelali, L.,Lachabi,A., (2026). Exploring Tl $_{1-x}$B $_x$As: A New Addition to the Family of Advanced Materials with Distinct Structural, Electronic and optical Properties. *J. Theor. Appl. Phys*., 20(1), 45-54. https://doi.org/10.57647/jtap.2026.2001.05

1. Introduction

In recent years, III–V semiconductor compounds have received considerable attention owing to their remarkable structural, electronic, and optical characteristics, which position them as strong contenders for advanced technological applications. Within this family, thallium (Tl)-based compounds and alloys have emerged as a distinct class of semiconductors that have been the focus of extensive theoretical and experimental investigations. A growing body of research has emphasized the potential of Tl–V materials for integration into optoelectronic and microelectronic devices such as photodetectors, diodes, and laser sources used in optical communication systems

[1,2]. For instance, Krishnamurthy et.al. [3] and Schilfgaarde et al. [4] explored the electronic properties of Tl-containing III–V compounds synthesized via molecular beam epitaxy (MBE). Houat et al. [5] examined the structural behavior of TlGaN alloys in the wurtzite phase, while Schilfgaarde et al. [4] identified TlInP as a promising candidate for infrared detection. Further contributions by Koh et al. [6] extended the investigation to ternary and quaternary alloys such as TlInP, TlGaP, and TlInGaP, whereas Takushima et al. [7] reported the successful growth of TlInAs alloys using low-temperature MBE. From a theoretical standpoint, Erden Gulebaglan [8] evaluated the electronic characteristics of $Tl_xAl_{1-x}As$ alloys crystallizing in the zinc blende phase within the framework of density functional theory (DFT), while Mankefors and Svensson [9] analyzed the structural and electronic properties of $Ga_{1-x}Tl_xAs$ alloys employing the local density approximation (LDA). Additionally, Schilfgaarde et al. [10] highlighted InTlP alloys as potential candidates for infrared detection, whereas Souza Dantas et al. [11] investigated the structural, electronic, and optical properties of $Al_{1-x}Tl_xN$ alloys within DFT, demonstrating their relevance for optoelectronic applications. Beyond the role of thallium in tailoring electronic and optical performance, boron (B) has recently emerged as a key element for engineering the properties of III–V semiconductors. Due to its small atomic radius and strong covalent bonding, boron incorporation can effectively modulate the lattice constant, band gap, and mechanical stability of semiconductor alloys. Previous studies have confirmed that boron doping not only enhances structural robustness but also introduces novel electronic and optical features desirable for next-generation optoelectronic technologies. Within this framework, the investigation of the ternary compound TlBAs at different boron concentrations (x = 0.25, 0.5, and 0.75) represents a significant step toward understanding the influence of boron on the electronic and optical responses of Tl-based materials, thereby opening new pathways for the design of innovative semiconductors for future device applications. Furthermore, the present study provides the first detailed insight into the effect of boron incorporation on the electronic nature of Tl-based III–V alloys. Our results demonstrate that the $Tl_{1-x}B_xAs$ alloy exhibits a remarkable composition-dependent electronic transition with increasing boron content. While the intermediate compositions (x = 0.0, 0.25, and 0.5) show semimetallic behavior with no band gap at the Fermi level, the system at x = 0.75, according to the improved mBJ-GGA approximation, begins to exhibit a direct band gap, indicating a progressive evolution in the electronic character of the compound. At the binary limit, BAs (x = 1), the material clearly reveals semiconducting behavior. This finding indicates that boron plays a crucial role in modulating the band topology and orbital interactions within the alloy system. The composition-dependent transition from metallic to direct and then indirect semiconducting behavior has not been reported previously for Tl–V–B systems, underscoring the novelty and scientific significance of the present work. The paper is organized as follows: The «method of calculation» section present a detailed description of the theoretical methodology adopted in the calculations. The « Results and discussion » section focuses on the analysis of the obtained results, including the study of structural, electronic, and optical properties of the investigated compounds. Finally, the «Conclusion» section summarizes the main findings and highlights the key outcomes of this study [55].

2. Calculation

To investigate the $Tl_xB_{1-x}As$ alloy in the zinc blende structure, a (2×2×2) super cells was constructed from the primitive cell of TlAs in the same structure, containing eight atoms. Partial substitution of thallium atoms by boron was performed to simulate different concentrations (x = 0.25, 0.50, and 0.75), corresponding to a substitutional alloy [13]. The substituted atomic sites were selected to minimize the loss of local symmetry, as this directly affects the total energy and, consequently, the structural stability and electronic properties of the compound. All calculations were carried out within the framework of density functional theory (DFT) using the WIEN2k code [12, 45, 46], based on the full-potential linearized augmented plane wave (FP-LAPW) method [47, 48]. The generalized gradient approximation (GGA) was employed to describe the exchange–correlation interactions [49, 50, 55]. To obtain a more accurate description of the electronic band structure and to correct the well-known underestimation of the band gap within GGA, the modified Becke–Johnson potential (mBJ-GGA) was also applied in a second step for the electronic and optical property calculations. The product of the smallest muffin-tin radius and the maximum plane-wave vector was set to Rmt·Kmax = 7.0 to ensure adequate convergence of the basis set. A dense k-point mesh of 1500 points (56 irreducible k-points) in the Brillouin zone was used, with an energy cutoff of −6 Ry. After atomic substitution, all structures were fully relaxed with respect to both lattice parameters and atomic positions until the residual forces on each atom became negligible. This procedure ensures the determination of the most energetically stable configuration in the zinc blende structure prior to the detailed analysis of the electronic and optical properties obtained within both GGA and mBJ-GGA approaches.

10.57647/jtap.2026.2001.05

The electronic valence configurations of the constituent atoms were treated as follows:

- Thallium (Tl): [Xe] $4f^{14}$ $5d^{10}$ $6s^2$ $6p^1$
- Boron (B): [He] $2s^2$ $2p^1$
- Arsenic (As): [Ar] $3d^{10}$ $4s^2$ $4p^3$

These configurations ensure an accurate description of the orbitals most relevant for interband optical transitions, particularly the Tl-6p states, which play a significant role in shaping the conduction band structure [14]. Finally, the optical response parameters were calculated for all studied compounds over the photon energy range of 0–14 eV. This computational setup provides a reliable framework for exploring the structural stability, electronic band dispersion, and optical behavior of $Tl_xB_{1-x}As$ alloys.

3. Results and discussion

3.1. Structural properties

In this section, we investigate the structural properties of the $Tl_{1-x}B_xAs$ alloy within the GGA framework. Ordered supercells containing eight atoms were constructed to represent different concentrations (x = 0.25, 0.5, 0.75) and periodically repeated in space. To determine the equilibrium lattice constants the total energies were calculated for a range of volumes and then fitted using the Murnaghan equation of state [15].

Our results reveal that the calculated lattice constants of the alloy do not strictly follow Vegard's law [16] ,which assumes a linear variation between the binary compounds (TlAs and BAs). As shown in Figure 1 the dependence of the lattice constant on composition exhibits a noticeable deviation from linearity, with a bowing parameter estimated at b ≈ – 0.10209 Å from the fitting procedure. The partial fits further indicate that the bowing values vary with composition, ranging between – 0.015720 Å and – 0.20147 Å. The negative sign of the bowing parameter corresponds to upward bowing, meaning that the computed lattice constants are slightly larger than those predicted by linear interpolation.

This deviation can be attributed to the significant difference between the lattice parameters of the binary compounds emphasizing the limitations of Vegard's law in describing this alloy. Therefore, it can be concluded that the $Tl_{1-x}B_xAs$ alloy similar to other semiconductor alloys where comparable deviations have been reported both experimentally [17] and theoretically [18] exhibits a nonlinear variation of the lattice constant with composition making the bowing parameter a key factor for accurately describing its structural behavior. The following form can approximate the lattice parameter data:

$$a_{TlBAs}(x) = xa_{BAs} + (1-x)a_{TlAs} - bx(1-x) \quad (1)$$

Figure 2 Shows the variation of the bulk modulus as a function of boron concentration x.

The results reveal that the bulk modulus increases with increasing boron content ($0 \leq x \leq 1$) indicating that the alloy becomes less compressible and mechanically stiffer as x approaches 1 (BAs). This behavior reflects the strengthening of the interatomic bonding due to the incorporation of boron atoms.

$$B_{TlBAs} = xB_{BAs} + (1-x)B_{TlAs} - bx(1-x) \quad (2)$$

The obtained results show a good agreement with the available theoretical and experimental data reported in the literature for both the lattice constant and the bulk modulus as summarized in Table 1.

This consistency demonstrates the accuracy and reliability of the present calculations performed within the GGA framework of density functional theory (DFT).

The calculated lattice constants are very close to those previously reported, with only minor deviations that can be attributed to differences in the exchange - correlation functionals or computational settings used in other studies such as the k-point mesh density of the Rmt·Kmax value.

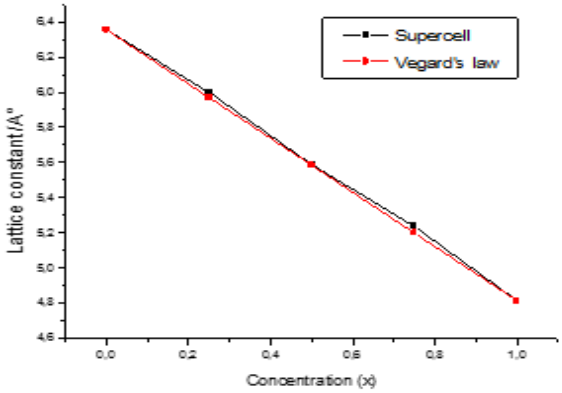

Figure 1. Composition dependence of the calculated lattice constant of $Tl_{1-x}B_xAs$ alloy compared with Vegard's law

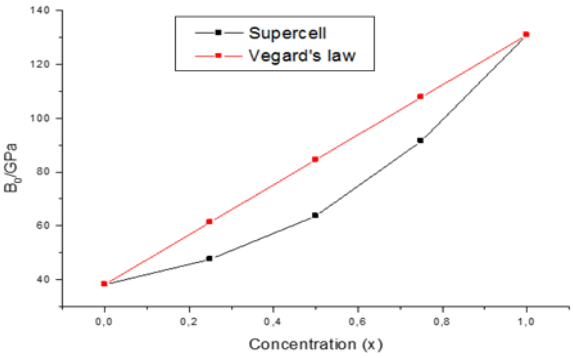

Figure 2. Composition dependence of the calculated bulk modulus of $Tl_{1-x}B_xAs$ alloy compared with Vegard's law

Table 1. Calculated lattice parameter (a) and bulk modulus (B) for Tl1-xBxAs alliy compounds. Available experimental and theoretical data from the literature are also included for comparison

Alloy	Parameters	
	a (A°)	B/GPa
TlAs (this work)	6.3548	38.1483
TlAs[14]	6.374[a]	37.196[a]
TlAs	6.170[e]	50.2[e]
TlAs	5.946[d]	49[d]
TlAs	6.088[f]	55.18[f]
$Tl_{0.75}B_{0.25}As$	5.99875	47.5806
$Tl_{0.5}B_{0.5}As$	5.58755	63.6617
$Tl_{0.25}B_{0.75}As$	5.236	91.4741
BAs (this work)	4.8127	130.9268
BAs	4.668[b]	154.30[b]
BAs	4.777[c]	145[c]
BAs	4.784[h]	137[h]
BAs	4.728[i]	144[i]
BAs (exp)	4.777[g]	-

[a] Ref[19], [b] Ref[20], [c] Ref[21], [d] Ref[22], [e] Ref[23],[f] Ref[24], [g] Ref[25],[h] Ref[26], [i] Ref[27]

Similarly, the obtained bulk modulus follows the same trend observed in earlier theoretical and experimental works, further confirming the robustness of the present structural results.

Overall, this agreement indicates that the adopted computational approach is sufficiently accurate to describe the structural properties of the studied alloy thereby providing strong confidence in the reliability of the subsequent electronic and optical analyses presented in this work.

Moreover, the slight deviations observed between the present results and previously reported data can also be attributed to the difference in atomic interactions and bonding character resulting from the partial substitution of B by Tl.

The incorporation of heavier Tl atoms with larger atomic radii tends to increase the lattice constant and slightly reduce the bulk modulus due to weaker covalent bonding strength.

This behavior is consistent with the general trend observed in III–V alloys, where increasing the cation size leads to a lattice expansion and lower compressibility.

3.2. Electronic properties

The electronic band structure calculations performed within the GGA approximation reveal that all the investigated compounds exhibit semimetallic behavior, with no distinct band gap at the Fermi level, except for the BAs compound, which displays an indirect band gap of about 1.20 eV.

In this material, the valence band maximum is located at the Γ point, while the conduction band minimum appears at the X point (Γ→X).This feature indicates that the electronic structure of BAs is governed by a different type of orbital hybridization compared to the other compounds, leading to its indirect semiconducting nature.

Conversely, the absence of a band gap in the remaining systems results from the overlap between the valence and conduction bands, which drives them toward semimetallic behavior.

Although it is well known that GGA tends to underestimate band gaps due to its limited ability to accurately describe the exchange correlation potential [28, 29], it remains a reliable and consistent approach for predicting qualitative electronic characteristics such as the nature of the band gap, the dispersion of bands, and the hybridization between atomic orbitals. GGA offers a balanced compromise between computational efficiency and accuracy, particularly suitable for comparative investigations and for systems containing heavy elements like thallium, where relativistic effects and spin orbit coupling already impose a significant computational cost. To improve the quantitative accuracy of the electronic band gap calculations, the modified Becke–Johnson (mBJ) potential [51] was also employed in this study. Interestingly, the mBJ–GGA results at a boron concentration of x = 0.75 revealed that the TlBAs compound undergoes a transition from semimetallic to direct semiconducting behavior, indicating that increasing the boron content significantly alters the orbital hybridization and redistributes the electronic states around the Fermi level. More sophisticated approaches such as hybrid functionals (HSE06) [52] or many-body GW corrections [53] could yield even more accurate quantitative predictions of band gaps; however, these are computationally demanding and not essential when the primary goal is to determine the qualitative electronic nature, as in the present work. Moreover, several previous theoretical studies have successfully applied the GGA approximation to describe the semimetallic and semiconducting behaviors of related III–V and thallium-based compounds, showing good agreement with experimental data, which supports the validity of this methodological choice. Accordingly, the combined GGA and mBJ results presented here are sufficient to clearly differentiate between BAs, which behaves as an indirect semiconductor, and the other $Tl_{1-x}B_xAs$ alloys that exhibit metallic or semimetallic features, with the notable exception of TlBAs at x = 0.75, showing a direct semiconducting character. Figures 3–5 highlight these distinctions by illustrating the band overlap in most systems and the indirect-to-direct energy gap evolution, thereby validating the qualitative and

quantitative accuracy of the adopted computational framework.

It is worth noting that the metallic or semimetallic behavior observed in most compounds arises mainly from the strong hybridization between atomic orbitals, which causes a broad dispersion of electronic states around and across the Fermi level.

In contrast, the emergence of an energy gap in BAs and the direct gap in TlBAs (x = 0.75) indicates weaker orbital interactions and a reduced overlap between the valence and conduction bands, leading to their semiconducting character [54]. No experimental or theoretical data are available to compare these predicted values.

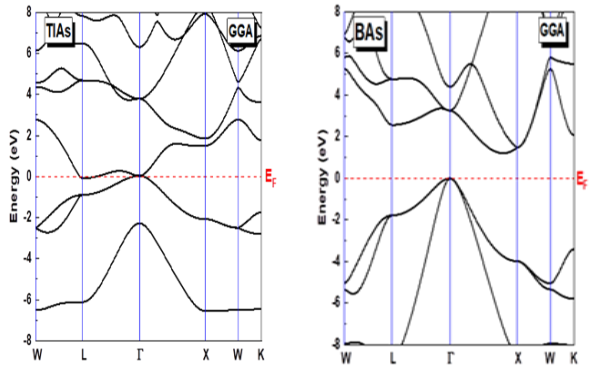

Figure 3. Band gap energy of TlAs and Bas compound calculated within GGA approximation . The horizontal dashed line indicates the Fermi level

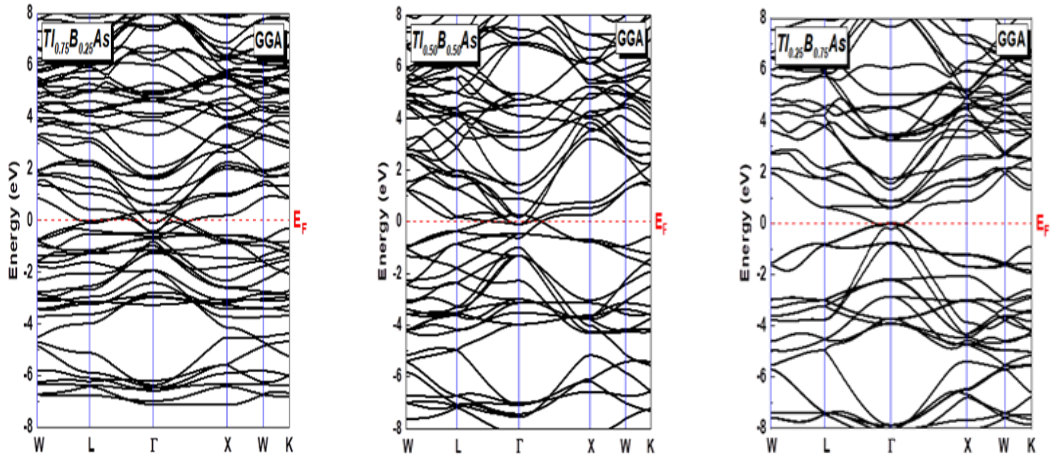

Figure 4. Variation of band gap energy for $Tl_{1-x}B_xAs$ ($0 \le x \le 1$) alloys calculated within the GGA approximation. The horizontal dashed line indicates the Fermi level

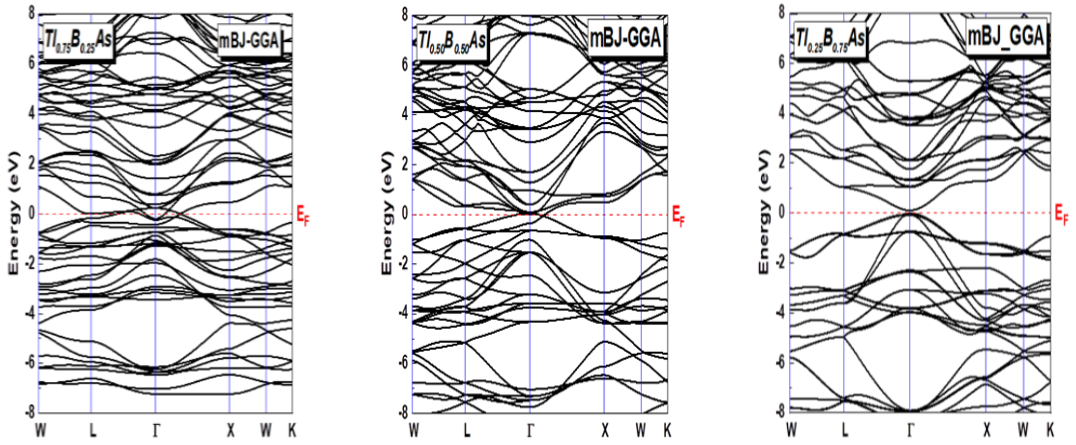

Figure 5. Variation of band gap energy for $Tl_{1-x}B_xAs$ ($0 \le x \le 1$) alloys calculated within the Mbj-GGA approximation. The horizontal dashed line indicates the Fermi level

The calculated energy gap values using the GGA and mBJ–GGA approximations are presented in Table 2.

In general, the trend shown in Table 2 indicates that increasing the boron content leads to a gradual transition from metallic to semiconducting behavior, with a small direct band gap appearing at intermediate compositions and a clear indirect gap at $x = 1$. Moreover, the obtained results show good agreement with the available literature, confirming the reliability of the mBJ approximation in improving the description of the electronic structure and correcting the well-known underestimation of the energy gap values obtained using conventional GGA.

Table 2. Calculated band gap energy for Tl1-xBxAs alloy

Alloy	Band Gap Eg (eV)		
	This work		Other calculations
	GGA	MbJ-GGA	
TlAs	~ 0.00	~ 0.00	~ 0.000 [a]
			~ 0.000 [b]
			~ 0.000 [c]
$Tl_{0.75}B_{0.25}As$	~ 0.00	~ 0.00	-
$Tl_{0.5}B_{0.5}As$	~ 0.00	~ 0.00	-
$Tl_{0.25}B_{0.75}As$	~ 0.00	0.10763	-
BAs	1.20819	1.71103	1.410 [d]
			1.460 [e]
			1.930 [f]
			1.220 [g]
			1.200 [h]
			1.210 [I]
			1.230 [j]
			1.250 [k]
			1.360 [l]
BAs (exp)			1.46 ind [m]
BAs (exp)			0.67 ind [n]

[a] Ref[30], [b] Ref[31], [c] Ref[32], [d] Ref[33], [e] Ref[34], [f] Ref[35], [g] Ref[36], [h] Ref[37], [i] Ref[38], [j] Ref[39], [k] Ref[40], [l] Ref[41], [m] Ref[42], [n] Ref[43]

3.3. Optical properties

The study of optical properties of solid materials is a fundamental tool for understanding the relationship between their electronic structure and their response to electromagnetic radiation. These properties are commonly described by the complex dielectric function:

$$\varepsilon(\omega) = \varepsilon_1(\omega) + i\varepsilon_2(\omega) \quad (3)$$

Where the imaginary part $\varepsilon_2(\omega)$ represents the contribution of allowed electronic transitions and is directly calculated using the joint density of states and the optical matrix elements. The real part $\varepsilon_1(\omega)$ can be derived from $\varepsilon_2(\omega)$ through the Kramers–Kronig relation [44].

This relationship provides a solid foundation for calculating other important optical functions notably the refractive index n(ω) which can be expressed as:

$$n(\omega) = \sqrt{\frac{\varepsilon(\omega) + i\varepsilon_1(\omega)}{2}} \quad (4)$$

In this work, these optical properties were investigated within the energy range from 0 eV to 14 eV allowing a detailed analysis of the variation of the dielectric function and the refractive index with energy.

This approach enables an in-depth understanding of the intrinsic optical behavior of the studied compounds and their potential applicability in technological devices such as optical components spectral filters and photovoltaic cells.

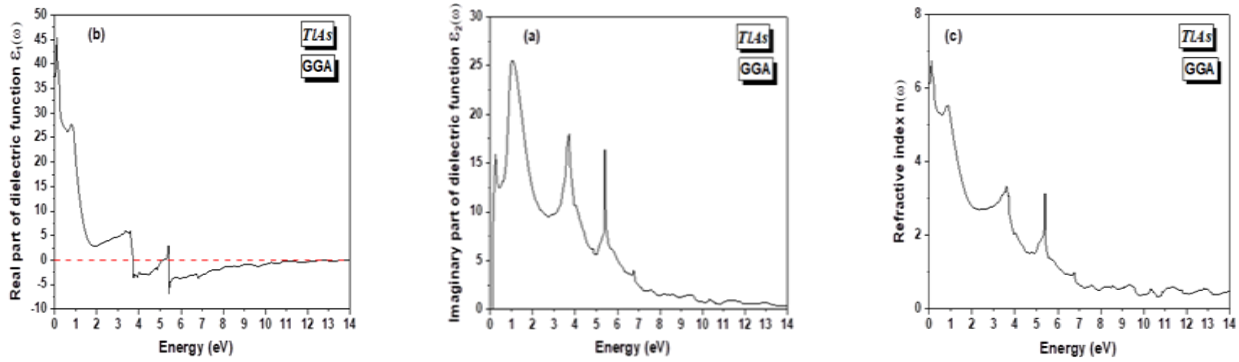

Figure 6. The calculated real $\varepsilon_1(\omega)$, imaginary $\varepsilon_2(\omega)$ parts of the dielectric functions, along with refractive index n(ω) for the TlAs compound as a function of photon energy

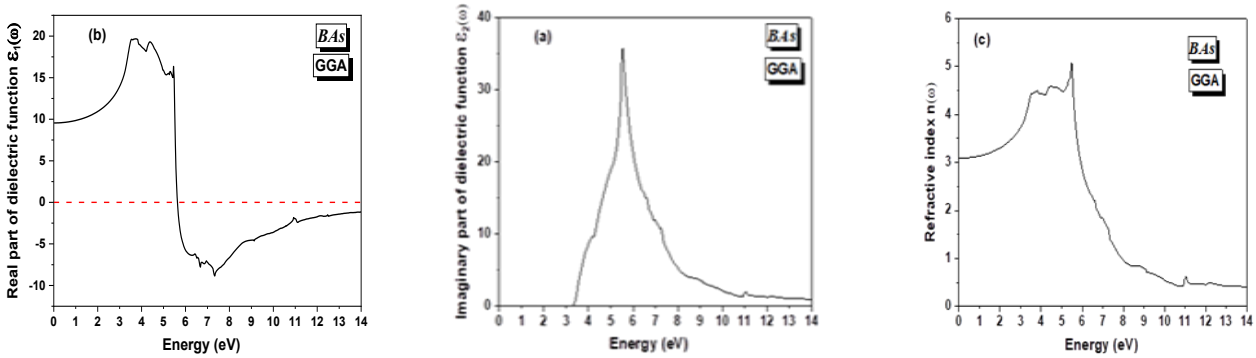

Figure 7. The calculated real $\varepsilon_1(\omega)$, imaginary $\varepsilon_2(\omega)$ parts of the dielectric functions, along with refractive index n(ω) for the BAs compound as a function of photon energy

10.57647/jtap.2026.2001.05

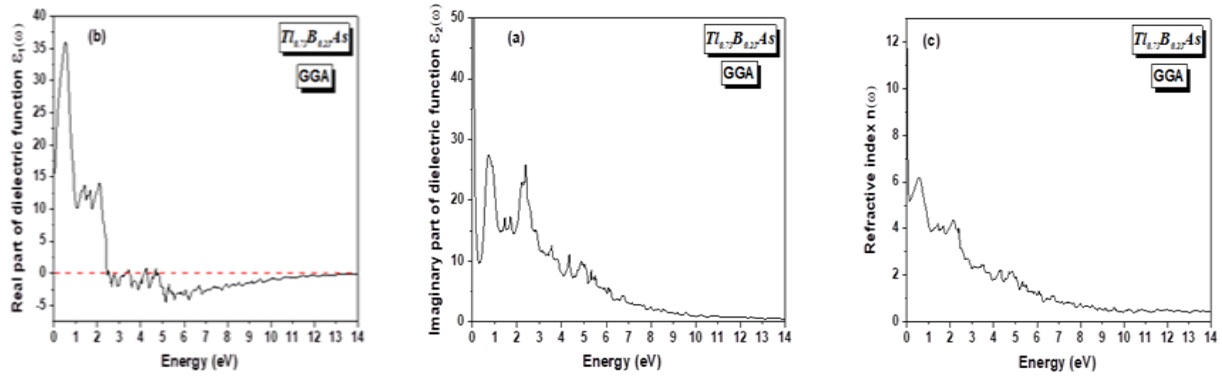

Figure 8. The calculated real $\varepsilon_1(\omega)$, imaginary $\varepsilon_2(\omega)$ parts of the dielectric functions, along with refractive index $n(\omega)$ for the $Tl_{.0.75}B_{0.25}As$ compound as a function of photon energy

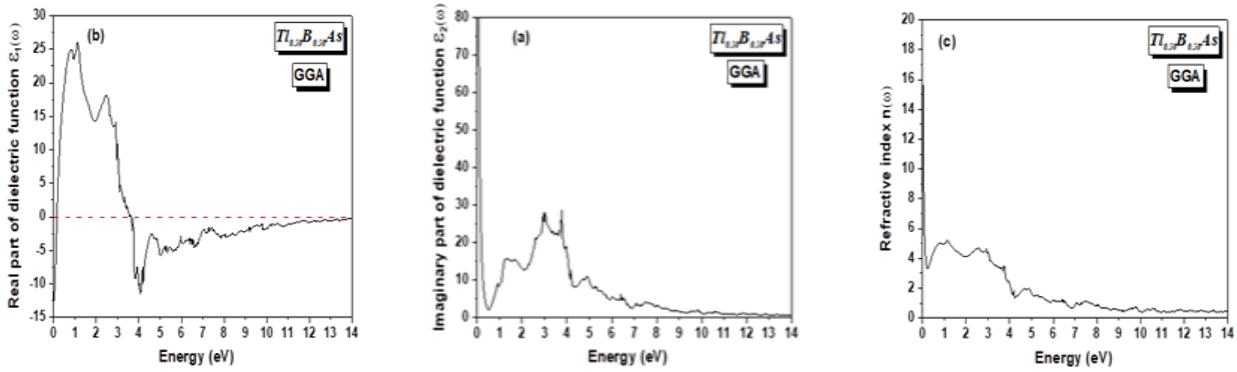

Figure 9. The calculated real $\varepsilon_1(\omega)$, imaginary $\varepsilon_2(\omega)$ parts of the dielectric functions, along with refractive index $n(\omega)$ for the $Tl_{0.5}B_{0.5}As$ compound as a function of photon energy

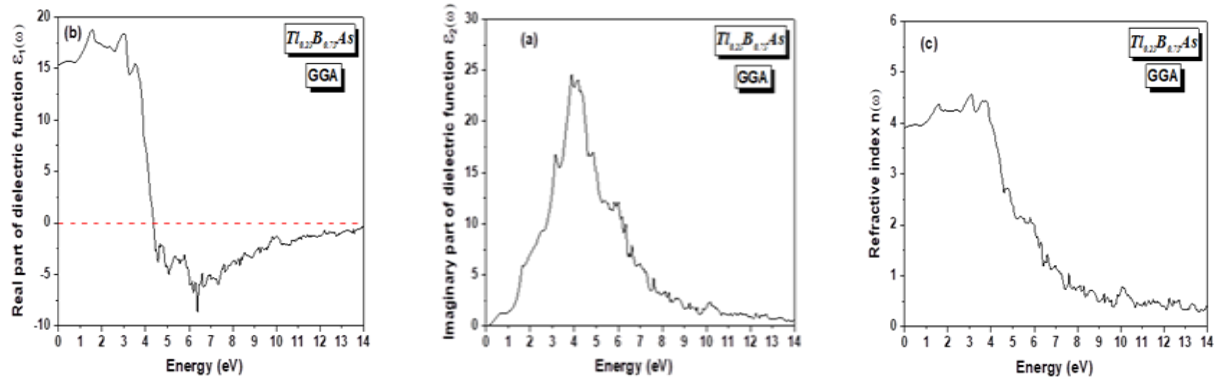

Figure 10. The calculated real $\varepsilon_1(\omega)$, imaginary $\varepsilon_2(\omega)$ parts of the dielectric functions, along with refractive index $n(\omega)$ for the $Tl_{0.25}B_{0.75}As$ compound as a function of photon energy

As shown in Figures 6, 7, 8, 9, and 10 the analysis of the real part of the dielectric function ε_1 (ω) for $Tl_{1-x}B_xAs$ alloys at different concentrations (x = 0, 0.25, 0.5, 0.75, and 1) reveals positive values with distinct maxima located at 0.2, 1, 2.3, 2.6, and 3.5 eV, respectively. The highest peak is observed for TlAs, reaching about 45 at very low photon energies. Regarding the imaginary part ε_2 (ω), the absorption begins at zero photon energy for all alloys except for BAs, where it starts around 3.2 eV, highlighting its semiconducting nature. The absorption maxima are recorded at 25 (1 eV) for TlAs, 35 (5.5 eV) for BAs, and at 27.5, 25, and 25 for x = 0.25, 0.5, and 0.75 at 0.75, 1.2, and 3 eV, respectively. These absorption peaks originate from interband electronic transitions between the occupied states in the valence band and the unoccupied states in the conduction band. The refractive index n (ω) shows a consistent trend with the real part of the dielectric function, where the maximum occurs at very low photon energies for TlAs (0 eV), while BAs exhibits its highest value at 5.5 eV. For intermediate concentrations (x = 0.25 and 0.5), the refractive index attains its maximum at photon energies close to zero, whereas for x = 0.75, the peak shifts toward approximately 3 eV. This behavior indicates that boron incorporation into the TlAs matrix significantly modifies the optical response, leading to a redistribution of absorption spectra and a tunable shift in the refractive

index peaks. Such tunability highlights the potential of $Tl_{1-x}B_xAs$ alloys for advanced optoelectronic applications, where precise control over refractive index and absorption properties is crucial. It is worth noting that this composition-dependent optical tunability has not been previously reported in TlBAs systems, highlighting the novel and original aspect of the present research work.

4. Conclusion

In this work, a comprehensive theoretical study of $Tl_{1-x}B_xAs$ ($0 \leq x \leq 1$) alloys in the zinc blende structure was conducted using density functional theory (DFT) within the GGA and mBJ approximations. The obtained results show excellent agreement with previous theoretical and experimental data, confirming the reliability of the adopted computational approach. The incorporation of boron into the TlAs lattice leads to a decrease in lattice constant and an increase in bulk modulus, indicating enhanced structural rigidity. Electronic structure calculations within GGA reveal that most compounds exhibit semimetallic behavior, except for BAs, which shows an indirect band gap (~1.20 eV). Interestingly, the mBJ correction indicates that at a boron concentration of x = 0.75, the $Tl_{0.25}B_{0.75}As$ alloy exhibits a direct semiconducting behavior, marking a notable and novel finding in this material system. Optical analyses show that the positions of the main peaks in the dielectric and refractive index spectra vary with boron content, reflecting a tunable optical response through compositional control. Overall, the present findings highlight that $Tl_{1-x}B_xAs$ alloys exhibit highly tunable electronic and optical characteristics, positioning them as promising candidates for next-generation optoelectronic and photonic devices

Acknowledgments

I would like to express my sincere gratitude to all those who supported and assisted me throughout the completion of this work. Particularly Prof Abdelhadi Lachabi and Prof Hamza Abid.

Authors Contribution
All the authors have participated sufficiently in the intellectual content, conception and design of this work or the analysis and interpretation of the data (when applicable), as well as the writing of the manuscript.

Availability of data and materials
The data that support the findings of this study are available from the corresponding author, upon reasonable request.

Conflict of interests
The author states that there is no conflict of interest.

References

[1] Saidi-Houat, N., Zaoui, A. and Ferhat, M., Structural stability of thallium-V compounds, Journal of Physics:Condensed Matter, 19, 106221/1–18 (2007). http://dx.doi.org/ 10.1088/0953-8984/19/10/106221

[2] Ferhat, M. and Zaoui, A., Do all III-V compounds have the zinc-blende or wurtzite ground state structure?, Applied Physics Letters, 88, 161902, (2006). http://dx.doi.org/10.1063/1.2196050

[3] Krishnamurthy, S., Chen A., B. and Sher, A., Near band edge absorption spectra of narrow-gap III–V semiconductor alloys, Applied Physics Letters, 80, 7, 4045-4048, (1996). https://doi.org/10.1063/1.363364

[4] Schilfgaarde, M.V., Chen, A.B., Krishnamurthy, S. and Sher, A., InTlP – a proposed infrared detector, Applied Physics Letters, 65, 2714-2716, (1994). https://doi.org/10.1063/1.112567

[5] Saidi-Houata, N., Zaoui, A., Belabbes, A., and Ferhat, M., Ab initio study of the fundamental properties of novel III–V nitride alloys Ga1−xTlxN, Materials Science and Engineering B, 162, 1, 26-31, (2009). https://doi.org/10.1016/j.mseb.2009.01.031

[6] Koh, H., Asahi, H., Fushida, M., Yamamoto, K., Takenaka, K., Asami, K., Gonda, S. and Oe, K., Photoconductance measurement on TlInGaP grown by gas source MBE, Journal of Crystal Growth, 188, 107-112, (1998). https://doi.org/10.1016/S0022-0248(98)00047-5

[7] Takushima, M., Kobayashi, N., Yamashita, Y., Kajikawa, Y., Satou, Y., Tanaka, Y. and Sumida, N., Thallium incorporation during TlInAs growth by low-temperature MBE, Journal of Crystal Growth,301-302, 117-120, (2007). https://doi.org/10.1016/j.jcrysgro.2006.11.141

[8] Erden Gulebaglan, S., The composition effect on the bowing parameter in the cubic TlxAl1-xAs, Modern Physics Letters B, 26, 30, 1250199-8, (2012). https://doi.org/10.1142/S0217984912501990

[9] Mankefos S. and Svensson S.P., Ab initio investigation of the electronic and geometric structure of Zincblende Ga1-xTlxAs alloys, Journal of Physics: Condensed Matter,12, 1223-1237, (2000). https://doi.org/10.1088/0953-8984/12/7/307

[10] Van Schilfgaarde M., Chen An-Ben, Krishnamurthy S. and Sher A., InTlP – a proposed infrared detector material, Applied Physics Letters, 65(12) (1994).

https://doi.org/10.1063/1.112567

[11] Souza Dantas N., de Almeida J.S., Ahuja R., Persson C. and Ferreira da Silva A., Novel semiconducting materials for optoelectronic applications: Al1-xTlxN alloys, Applied Physics Letters, 92, 121914, (2008). https://doi.org/10.1063/1.2901146

[12] Blaha,P, Schwarz ,k ;Madsen .G.K.H,kvasnicka ,D&Luitz , J (2001).WIEN2K:An augmented Plane Wave +Local Orbitals program for calculating Crystal Properties.Vienna university of technology .Available at: http://www.wien2k.at

[13] Masek,J,Kudrnovsky , J.Maca ,F ,Drchal , V&Turek , l (2003) .Lattice constant in diluted magnetic semiconductors (Ga, Mn)As. physical Review B 67(15), 153203. https://doi.org/10.1103/PhysRevB.67.153203

[14] Lannoo ,M & Bourgion , J .(1981).Point Defects in Semiconductors l :Theoretical Aspects .Spring Seeries in solid-State sciences, Vol22,springer-Verlag ISBN:978-3-540-10868-5

[15] Murnaghan, F. D. (1944). The compressibility of media under extreme pressures. Proceedings of the national Academy of Sciences, 30(9), 244-247. https://www.Pnas.org by 154.121.40.225

[16] L. Vegard, Z. Phys.5 (1921) 17. https://doi.org/10.1007/BF01349680

[17] J. Jobst, D. Hommel, U. Lunz, T. Gerhard and G. Landwehr, Appl. Phys. Lett. 69 (1996) 97. https://doi.org/10.1063/1.118132

[18] F. Elhaj hassan, Phys. Stat. Sol. (b)242 (2005) 909. https://doi.org/10.1002/pssb.200402110

[19] A. El Hassasna and A. Bechiri, 'Electronic and Elastic Properties of TlX (X = N, P, As and Sb) in Zinc-Blende Structure', Solid State Phenom., vol. 297, pp. 82–94, Sep.2019. https://doi.org/10.4028/www.scientific.net/SSP.297.82

[20] K. Bencherif, A. Yakoubi, and H. Mebtouche, 'Structural and Electronic Properties of the BN, BP and BAs in the Different Phases of Zinc-Blende, NaCl and CsCl', Acta Phys. Pol. A, vol. 131, no. 1, pp. 209–212, Feb. 2017. https://doi.org/10.12693/APhsPolA.131.209

[21] R. M. Wentzcovitch, M. L. Cohen, and P. K. Lam, 'Theoretical study of BN, BP, and BAs at high pressures', Phys. Rev. B, vol. 36, no. 11, p. 6058, 1987. https://doi.org/10.1103/PhysRevB.36.6058

[22] S. Q. Wang, H. Q. Ye, Phys. Rev. B 66, 235111 (2002) https://doi.org/10.1103/PhysRevB.66.235111

[23] Mazzouz H M, Belabbes A, Zaoui A and Ferhat M 2010. Superlatices and Microstructures 48 560. https://doi.org/10.1016/j.spmi.2010.09.012

[24] Zhou J, Ren X M, Hung Y Q, Wang Q and Hung H 2008 Chin. Phy. Lett. 25 3353. https://ui.adsabs.harvard.edu/link_gateway/2008ChPhL.25.3353Z/doi:10.1088/0256-307X/25/9/069

[25] S. Adachi, Properties of Group IV, III–V and II–VI Semiconductors, Departement of Electronic Engineering, Gumma University, Japan, 2005. ISBN: 0-470-09032-4 (Hb)

[26] A. Zaoui and F. Elhaj Hassan, J. Phys: Condens.Matter 13 (2001) 253. https://doi.org/ 10.1088/0953-8984/13/2/303

[27] B. Bouhafs, H. Aourag, M. Ferhat and M. Certier, J. Phys: Condens.Matter 12 (2000) 5655. PII: S0953-8984(00)07643-8

[28] P. Hohenberg and W. Kohn, Physical Review, 136, B864 (1964). https://doi.org/10.1103/PhysRev.136.B864

[29] J. P. Perdew, K. Burke, and M. Ernzerhof, Physical Review Letters, 77, 3865 (1996). https://doi.org/10.1103/PhysRevLett.77.3865

[30] Sinem E. Gulebaglan_, Emel K. Dogan, Murat Aycibin, Mehmet N. Secuk, Bahattin Erdinc, Harun Akkus . Cent. Eur. J. Phys. 11(12) . 2013. 1680-1685. https://doi.org/10.2478/s11534-013-0314-1

[31] Phys.:Condens. Matter 19, 106221 (2007). https://doi.org/10.1088/0953-8984/19/10/106221

[32] S. Q. Wang, H. Q. Ye, Phys. Rev. B 66, 235111 (2002). https://doi.org/10.1103/PhysRevB.66.235111

[33] M. Guemoua,, B.Bouhafs , A.Abdiche , R.Khenata , Y.AlDouri , S.BinOmran . Physica B 407 (2012) 1292–1300. https://doi.org/10.1016/j.physb.2012.01.132

[34] V.M. Daniel'tsev, N.V. Vostokov, Yu.N. Drozdov, M.N. Drozdov, A.V. Murel, D.A. Pryakhin, O.I. Khrykin, V.I. Shashkin, J. Surf. Invest. 2 (4) (2008) 514. https://doi.org/10.1016/j.physb.2012.01.132

[35] N. Chimot, J. Even, H. Folliot, S. Loualiche, Physica B 364 (2005) 263. https://doi.org/10.1016/j.physb.2005.04.022

[36] M. Merabet, D. Rached, R. Khenata, S. Benalia, B. Abidri, N. Bettahar, S. Bin Omran, Physica B 406 (2011) 3247.

https://doi.org/10.1016/j.physb.2011.05.034

[37] H. Meradji, S. Labidi, S. Ghemid, S. Drablia, B. Bouhafs, Phys. Procedia 2 (2009) 933. https://doi.org/10.1016/j.phpro.2009.11.046

[38] H. Meradji, S. Drablia, S. Ghemid, H. Belkhir, B. Bouhafs, and A. Tadjer, 'First-principles elastic constants and electronic structure of BP, BAs, and BSb', Phys. Status Solidi B, vol. 241, no. 13, pp. 2881–2885, Nov. 2004, https://doi.org/10.1002/pssb.200302064

[39] Sinem E. Gulebaglan, Emel K. Dogan, Murat Aycibin, Mehmet N. Secuk, Bahattin Erdinc, Harun Akkus. Cent. Eur. J. Phys. 11(12). 2013. 1680-1685. https://doi.org/10.2478/s11534-013-0314-1

[40] R. M. Wentzcovitch, M. L. Cohen, and P. K. Lam, 5'Theoretical study of BN, BP, and BAs at high pressures', Phys. Rev. B, vol. 36, no. 11, p. 6058, 1987. https://doi.org/10.1103/PhysRevB.36.605

[41] Elisangela da Silva Barboz, Alex andrec. Dias, Luis Graco, Sabrina S. Carara, Diegor. Da Costa and Teldo A. S. Pereira.Electronic, excitonic, and optical properties of zinc blende boron arsenide tuned by hydrostatic pressure. ACS Omega (2024), 9, 47710-47718. https://doi.org/10.1021/acsomega.4c07598

[42] Zaoui 1.and F.El Haj Hassan, J.phys condens matter 13, p253.(2001). https://doi.org/10.1088/0953-8984/13/2/303

[43] M. Rabah, B. Abbar, Y. Al-Douri, B. Bouhafs, B. Sahraoui, Mater. Sci. Eng. B 100 (2003) 163. https://doi.org/10.1016/S0921-5107(03)00093-X

[44] S. Alnujaim; A. Bouhemadou, M. Chegaar, A. Guechi, S. Bin-Omran, R. Khenata, Y. Al-douri, W. Yang. H. Lu, The European Physical Journal B 95, 114 (2022). https://doi.org/10.1140/epjb/s10051-022-00381-2

[45] Karlheinz Schwarz, Peter Blaha, Georg KH Madsen, Electronic structure calculations of solids using the WIEN2k package for material sciences, Comput. Phys. Commun. 147 (1–2) (2002) 71–76. https://doi.org/10.1016/S0010-4655(02)00206-0

[46] Shiwu Gao, Linear-scaling parallelization of the WIEN package with MPI, Comput. Phys. Commun. 153 (2) (2003) 190–198. https://doi.org/10.1016/S0010-4655(03)00224-8

[47] Karlheinz Schwarz, DFT calculations of solids with LAPW and WIEN2k, J. Solid State Chem. 176 (2) (2003) 319–328. https://doi.org/10.1016/S0022-4596(03)00213-5

[48] Blaha Peter, Karlheinz Schwarz, Georg K.H. Madsen, Dieter Kvasnicka, and Joachim Luitz. "wien2k." An augmented plane wave+ local orbitals program for calculating crystal properties (2001). ISBN 3-9501031-1-2|

[49] John P. Perdew, Kieron Burke, Matthias Ernzerhof, Generalized gradient approximation made simple, Phys. Rev. Lett. 77 (18) (1996) 3865. https://doi.org/10.1103/PhysRevLett.77.3865

[50] John P. Perdew, Alex Zunger, Self-interaction correction to density-functional approximations for many-electron systems, Phys. Rev. B 23 (10) (1981) 5048. https://doi.org/10.1103/PhysRevB.23.5048

[51] F. Tran and P. Blaha, Physical Review Letters, 102, 226401 (2009). https://doi.org/10.1103/PhysRevLett.102.226401

[52] J. Heyd, G. E. Scuseria, and M. Ernzerhof, Journal of Chemical Physics, 118, 8207 (2003). https://doi.org/10.1063/1.1564060

[53] A. Rubio and M. L. Cohen, Physical Review B, 51, 4343 (1995). https://doi.org/10.1103/PhysRevB.51.4343

[54] Nazir Ahmad Teli, M. Mohamed Sheik Sirajuddeen, Journal of Magnetism and Magnetic Materials 511 (2020) 166829. https://doi.org/10.1016/j.jmmm.2020.166829

[55] M. Mohamed Sheik Sirajuddeen • I. B. Shameem Banu. J Mater Sci. https://doi.org/10.1007/s10853-014-8705-2